NATIONAL ADVISORY COMMITTEE FOR AERONAUTICS

TECHNICAL NOTE 2551

EFFECT OF VARIOUS PARAMETERS INCLUDING MACH NUMBER ON THE SINGLE-DEGREE-OF-FREEDOM FLUTTER OF A CONTROL SURFACE IN POTENTIAL FLOW

By Harry L. Runyan

Langley Aeronautical Laboratory
Langley Field, Va.

Washington
December 1951

NATIONAL ADVISORY COMMITTEE FOR AERONAUTICS

TECHNICAL NOTE 2551

EFFECT OF VARIOUS PARAMETERS INCLUDING MACH NUMBER ON THE SINGLE-DEGREE-OF-FREEDOM FLUTTER OF A CONTROL SURFACE IN POTENTIAL FLOW

By Harry L. Runyan

SUMMARY

Various investigations of single-degree-of-freedom pitching oscillations of a wing in potential flow have been made. However, corresponding studies of single-degree-of-freedom flutter of a control surface have not been made. The present paper demonstrates by theoretical calculations that single-degree-of-freedom control-surface flutter is possible. The effects of structural damping, aerodynamic balance, axis of rotation, and compressibility are included.

The mechanism of instability presented here is based on potential-flow theory and the results of such a study are not directly applicable to separated flow; in addition, certain practical limitations are discussed.

INTRODUCTION

Flutter of a control surface alone, that is, an unstable oscillation in which the control surface is effectively rigid and nondeformable and rotates around its hinge line, has been encountered on aircraft in flight. This phenomenon, as well as stall flutter, is thought to be associated with separated or nonpotential flow, although the explanation is not entirely clear. Flutter of a control surface in one degree of freedom is possible in potential flow, at least theoretically, and forms the subject of the present paper. The development of this subject may possibly contribute to the understanding of the nonpotential-flow problem.

Theoretical investigations of several types of undamped single-degree-of-freedom oscillations in potential flow have been reported recently. For instance, Smilg (reference 1) has reported a study of the undamped oscillations of a pitching wing in incompressible flow and

this study has been extended by Runyan in reference 2 to include the effect of compressibility. Cunningham (reference 3) has studied the undamped bending oscillations of a swept wing in subsonic flow. The undamped pitching oscillations of a wing in supersonic flow have been studied by a number of investigators, for instance, Garrick and Rubinow (reference 4), Temple and Jahn (reference 5), and Watkins (reference 6).

The aforementioned papers concern single-degree-of-freedom pitching of a wing or the bending of a swept wing. Some examples of control-surface flutter in one degree of freedom are given in reference 7 along with a discussion of some possible causes. Apparently no calculation studies exist demonstrating the conditions for the existence of single-degree-of-freedom oscillations of a control surface. Accordingly, the purposes of this paper are (1) to show the conditions for the existence of single-degree-of-freedom oscillations of a control surface based on potential-flow theory and (2) to examine and present the effect of various parameters such as Mach number, fluid density (or altitude), location of axis of rotation, structural damping, and aerodynamic balance on this type of oscillatory instability.

Certain limitations which may affect practical consideration of the results presented in this paper should be noted: (1) the calculations are based on two-dimensional aerodynamic coefficients, and the effect of aspect ratio, which could be appreciable, is not taken into account, (2) the influence of additional degrees of freedom, which will always be present in actual configurations, is not considered, and (3) the effect of finite thickness and shape of the control surface is not considered, since the control surface has been replaced in theory by its mean camber line. In addition to these limitations, the results of this study are not directly applicable to separated flow, since the analysis was based on potential-flow theory. Nevertheless, this approach should provide a basis for comparison and study and a guide for further investigation.

SYMBOLS

b	wing half-chord, feet
c	location of hinge axis of control surface without aerodynamic balance with respect to midchord point, based on half-chord and positive rearward
c'	location of leading edge of control surface with aerodynamic balance with respect to midchord point, based on half-chord and positive rearward

C_β	torsional stiffness of control surface about hinge line c
c_{RR}	function of ratio of aileron chord to wing chord
e	location of hinge axis of control surface with aerodynamic balance with respect to midchord point, based on half-chord and positive rearward
F and G	transcendental functions of k for oscillating plane flow
g_β	structural damping coefficient ($\pi g_\beta \approx$ Logarithmic decrement)
$I_{b\beta}$	out-of-phase aerodynamic moment coefficient
$\bar{I}_{b\beta}$	total out-of-phase moment coefficient
I_β	mass moment of inertia of control surface about hinge line per unit length
K'_{RR} and K''_{RR}	aerodynamic moment coefficients for a control surface in compressible flow
k	reduced-frequency parameter ($b\omega/v$)
l	nondimensional distance from control-surface axis of rotation to leading edge of control surface (e - c')
M	Mach number
M_β	total complex aerodynamic moment on control surface
N_5, N_6	aerodynamic coefficients for a control surface in supersonic flow
$\bar{R}_{b\beta}$	total inphase moment coefficient
$R_{b\beta}'$	part of inphase aerodynamic moment on control surface
T_n	control-surface coefficients defined in references 8 and 9
v	flutter velocity, feet per second
β	control-surface rotation, measured from wing chord line

ρ fluid density, slugs per cubic foot

ω flutter frequency, radians per second

ω_β natural frequency of control surface about hinge axis, radians per second

ANALYSIS

In this section, the expression for the equilibrium of moments on a control surface oscillating about its hinge line is given, followed by a discussion of the aerodynamic moment for (1) a control surface oscillating in incompressible flow, (2) a control surface, having aerodynamic balance, oscillating in incompressible flow, and (3) a control surface oscillating in compressible flow.

The equation representing the equilibrium of moments per unit length on a control surface oscillating about the hinge line c is

$$I_\beta \ddot{\beta} + (1 + ig_\beta)C_\beta \beta = M_\beta \qquad (1)$$

where I_β is the mass moment of inertia per unit length of the control surface about its hinge line c, β is the angular deflection of the control surface measured from the chord line, g_β is a structural damping coefficient, and C_β is the torsional stiffness of the control system about c. The quantity M_β is a complex aerodynamic moment, which is a function, in part, of the displacement β, velocity $\dot{\beta}$, acceleration $\ddot{\beta}$, reduced-frequency parameter k, Mach number M, and location of hinge axis c. The complex notation has been in use in flutter work for many years because of its convenience, since it contains both the magnitude of the forces or moments and the phase with respect to the displacement. The expression for the aerodynamic moment M_β is given in reference 8 for a control surface which is hinged at its leading edge and oscillating in incompressible two-dimensional flow. An expression for the aerodynamic moment M_β for an aerodynamically balanced control surface is given in reference 9. Closed expressions for M_β for compressible fluid do not exist and values of the aerodynamic moment M_β must be obtained by use of tables as given, for example, in references 10 and 11 for subsonic flow ($M < 1$) and in reference 12 for supersonic flow ($M > 1$).

Since equation (1) is complex, it can be separated into two components as follows:

$$\bar{R}_{b\beta} + i\bar{I}_{b\beta} = 0 \tag{2}$$

where $\bar{R}_{b\beta}$ represents the inphase (real) moment coefficient and $\bar{I}_{b\beta}$ represents the out-of-phase moment coefficient for the control surface. Equation (2) implies that both components, $\bar{I}_{b\beta}$ and $\bar{R}_{b\beta}$, must vanish simultaneously for equilibrium.

The vanishing of the out-of-phase moment $\bar{I}_{b\beta}$ corresponds to a borderline condition between damped and undamped oscillations as was more fully discussed in reference 2. The flutter frequency may then be determined from the inphase (real) moment equation. This inphase moment equation $\bar{R}_{b\beta} = 0$ may be put in more convenient form as follows:

$$\left(\frac{\omega}{\omega_\beta}\right)^2 = \frac{1}{1 - R_{b\beta}' \frac{\pi\rho b^4}{\bar{I}_\beta}} \tag{3}$$

where $R_{b\beta}'$ is proportional to the inphase aerodynamic moment on the control surface. In the subsequent sections, expressions for $\bar{I}_{b\beta}$ and $R_{b\beta}'$ will be given for the various cases.

Equations for Incompressible Flow

Control surface without aerodynamic balance.- The expression for the aerodynamic moment on a harmonically oscillating control surface in incompressible flow having no aerodynamic balance may be derived from reference 8 as

$$M_\beta = -\rho b^2\left[\frac{1}{\pi} v^2\left(T_5 - T_4T_{10}\right)\beta - \frac{1}{2\pi} vb\dot{\beta}T_4T_{11} - \frac{1}{\pi} T_3b^2\ddot{\beta}\right] -$$

$$\rho vb^2T_{12}(F + iG)\left(\frac{1}{\pi} T_{10}v\beta + \frac{b}{2\pi} T_{11}\dot{\beta}\right) \tag{4}$$

where the T coefficients are functions only of the hinge position c and are defined in reference 9. Substitution of equation (4) into equation (1) and separation into the two components lead to equation (2) where

$$\bar{R}_{b\beta} \equiv \frac{T_3}{\pi^2} + \frac{1}{k^2\pi^2}\left(T_5 - T_4T_{10}\right) - \frac{T_{12}}{2\pi}\left(\frac{T_{11}}{2\pi}\frac{2G}{k} - \frac{T_{10}}{\pi}\frac{2F}{k^2}\right) + \frac{I_\beta}{\pi\rho b^4}\left[\left(\frac{\omega_\beta}{\omega}\right)^2 - 1\right]$$

$$= 0 \tag{5}$$

and

$$\bar{I}_{b\beta} \equiv \frac{1}{k}\left[\frac{T_{12}}{2\pi}\left(\frac{T_{10}}{\pi}\frac{2G}{k} + \frac{T_{11}}{2\pi}2F\right) - \frac{1}{2\pi^2}T_4T_{11}\right] + g_\beta\frac{I_\beta}{\pi\rho b^4}\left(\frac{\omega_\beta}{\omega}\right)^2$$

$$= 0 \tag{6}$$

The inphase (real) moment $\bar{R}_{b\beta}$ may be expressed in the form given by equation (3) where

$$R_{b\beta}' = -\frac{T_{12}}{2\pi}\left(\frac{T_{11}}{2\pi}\frac{2G}{k} - \frac{T_{10}}{\pi}\frac{2F}{k^2}\right) + \frac{T_3}{\pi^2} + \frac{1}{k^2\pi^2}\left(T_5 - T_4T_{10}\right) \tag{7}$$

A numerical or a graphical method is necessary for the solution of the out-of-phase moment $\bar{I}_{b\beta} = 0$ since the functions F and G are transcendental functions of 1/k. Once the combination of 1/k and F and G that satisfies equation (6) has been determined, the frequency and flutter speed can be obtained from equation (3) in which the value of $R_{b\beta}'$ is taken for the same value of 1/k that satisfied equation (6).

Control surface with aerodynamic balance.- The force and moment on a harmonically oscillating control surface having aerodynamic balance have been derived in reference 9 for incompressible flow. A control surface having aerodynamic balance is represented in reference 9 as follows:

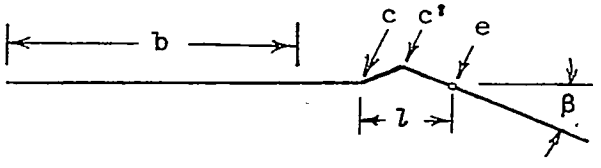

where the dimensions c, c', e, and l are referred to the half-chord b.

The out-of-phase (imaginary) moment coefficient may be derived from reference 9 as

$$I_{b\beta} \equiv \frac{1}{k}\left\{\frac{1}{\pi^2}\left(T_{19} + lT_{27} + l^2T_{29}\right) + \frac{1}{2\pi}\left(T_{12} - 2lT_{20}\right)\left[\frac{1}{\pi}\left(T_{10} - lT_{21}\right)\frac{2G}{k} + \frac{1}{2\pi}\left(T_{11} - 2lT_{10}\right)2F\right]\right\} = 0 \tag{8}$$

and the frequency is determined from the inphase (real) moment expressed as equation (3) where

$$R_{b\beta}' = -\frac{1}{\pi^2}\left(-T_3 + 2lT_2 - l^2T_5\right) + \frac{1}{k^2\pi^2}\left(T_{18} + lT_{26} + l^2T_{28}\right) - \frac{1}{2\pi}\left(T_{12} - 2lT_{20}\right)\left[\frac{1}{2\pi}\left(T_{11} - 2lT_{10}\right)\frac{2G}{k} - \frac{1}{\pi}\left(T_{10} - lT_{21}\right)\frac{2F}{k^2}\right] \tag{9}$$

The T coefficients are given in the appendix of reference 9 and all T's are functions of c. One exception that needs separate consideration is the term T_{28} which is discussed in reference 9. For the case (over idealized) of a sharp vertical step, the term T_{28} becomes infinite; however, for practical configurations certain approximations can be made which permit a finite-value determination of this term. One such simple approximation is given in reference (9) as

$$c' = \frac{1}{4}(e + 3c)$$

Equations for Compressible Flow

Closed expressions for aerodynamic moment and lift on oscillating wings and control surfaces in compressible flow do not exist. Aerodynamic moment and lift coefficients have been calculated by several investigators for various ranges of Mach number and reduced frequency and are usually presented in the form of tables. In reference 10,

tables of aerodynamic coefficients are presented for one aileron-to-wing-chord ratio of 15 percent ($c = 0.7$) for $M = 0.7$. These tables are extended in reference 11 to include several aileron-to-wing-chord ratios of 24, 33, and 42 percent.

A notation differing from that used in this paper is used in references 10 and 11 where the inphase (real) moment coefficient of a control surface is denoted by K'_{RR} and the damping (out-of-phase) moment is denoted by K''_{RR}. The relation between the coefficients of this paper and those of references 10 and 11 is given as

$$I_{b\beta} \equiv \frac{K''_{RR}}{k^2} = 0 \tag{10}$$

$$R_{b\beta}' \equiv \frac{K'_{RR}}{k^2} - c_{RR}$$

where c_{RR} is a function of the ratio of the aileron chord to the wing chord and is given in reference 11, page 16.

In order to obtain a solution, it is necessary to plot K''_{RR} against k and determine the value of k at which $K''_{RR} = 0$. The frequency is then given for the same value of $1/k$ by

$$\left(\frac{\omega}{\omega_\beta}\right)^2 = \frac{1}{1 - \left(\frac{K'_{RR}}{k^2} - c_{RR}\right)\frac{\pi\rho b^4}{I_\beta}} \tag{11}$$

The results of calculations of aerodynamic coefficients for a control surface oscillating in supersonic flow have been reported in reference 12. The aerodynamic moment on the control surface is given as

$$M_\beta = -4\rho b^2 v^2 k^2 \beta \left(N_5 + iN_6\right) \tag{12}$$

where N_5 is the inphase moment coefficient and N_6 is the out-of-phase moment coefficient. In order to obtain a solution for the out-of-phase moment, $N_6 = 0$, the value of $1/k$ at which $N_6 = 0$ must be

determined. The frequency is then given for the same value of $1/k$ by

$$\left(\frac{\omega}{\omega_\beta}\right)^2 = \frac{1}{1 - N_5 \frac{4}{\pi} \frac{\pi\rho b^4}{I_\beta}} \tag{13}$$

DISCUSSION OF RESULTS

In this section, the results of calculations based on the expressions previously presented are given. The oscillation of a control surface in incompressible flow with zero structural damping is discussed and the effect of structural damping is introduced. A discussion of the effect of aerodynamic balance and the effect of compressibility follows.

Flutter of control surface with zero structural damping in incompressible flow.- Calculations based on equations (5) and (6) where $g_\beta = 0$ have been made for various locations of the control-surface axis of rotation. The results of the computations are presented in figures 1 and 2 for ratios of the control-surface chord to wing chord of 10 percent, 30 percent, 50 percent, and 100 percent ($c = 0.8$, 0.4, 0, and -1).

In figure 1 the flutter-speed parameter $v/b\omega_\beta$ is plotted against an inertia parameter $I_\beta/\pi\rho b^4$. The curves represent the transition, for a given Mach number, from a damped or stable condition to an undamped or unstable condition. The stable region is below or to the left of a curve, and the unstable region is above or to the right of a curve. For small values of the inertia parameter the control surface would be stable and, if the inertia parameter is increased, for instance by an increase in altitude, a value equal to the vertical asymptote could be reached or exceeded. In figure 1(a) ($c = 0.8$) this value is $\frac{I_\beta}{\pi\rho b^4} = 7.58$ which increases to 577.7 (fig. 1(d)) for $c = -1.0$, that is, for a wing oscillating about its leading edge. The flutter speed for values of $I_\beta/\pi\rho b^4$ equal to the asymptote is infinite, but a slight increase in $I_\beta/\pi\rho b^4$ would result in a very rapid decrease in the flutter speed. For values of $I_\beta/\pi\rho b^4$ approaching infinity, $v/b\omega_\beta$ approaches a value equal to $v/b\omega$ at which the oscillation occurs. It should be noted that the oscillation occurs at a constant value of $v/b\omega$, which

means that, no matter what the value of the inertia parameter, the wave length of the oscillating wake will be the same in the border condition.

The frequency ratio $(\omega/\omega_\beta)^2$ is plotted against the inertia parameter $I_\beta/\pi\rho b^4$ in figure 2 for the same axis-of-rotation locations as for figure 1. The unstable region is above or to the right of a curve. The vertical asymptotes are the same as for figure 1, but the horizontal asymptote is unity. This fact indicates that, for very large values of $I_\beta/\pi\rho b^4$, the frequency of oscillation approaches the natural (still air) frequency of the control surface.

In figure 3, the value of the reduced velocity $1/k$ is plotted against the location of the axis of rotation of the control surface. Note that the variation of $1/k$ with c is not very large $(25 < 1/k < 35)$, but the values are considerably higher than experienced in flutter and approach values found in stability work.

In figure 4, the minimum value of the inertia parameter (vertical asymptote) at which the oscillation could occur is plotted against location of control-surface axis of rotation. The value of the inertia parameter increases as the aileron-to-wing-chord ratio increases. This plot is of particular significance with regard to the zero structural restraint case $(\omega_\beta = 0)$. If equation (3) is inverted to obtain

$$\left(\frac{\omega_\beta}{\omega}\right)^2 = 1 - R_{b\beta}' \frac{\pi\rho b^4}{I_\beta}$$

and $\omega_\beta = 0$, there is obtained the relation

$$R_{b\beta}' = \frac{I_\beta}{\pi\rho b^4} \tag{14}$$

which indicates that, if $I_\beta/\pi\rho b^4$ is equal to $R_{b\beta}'$, an oscillation is possible. The frequency of oscillation is then a direct function of the velocity, and flutter can theoretically occur above zero airspeed as shown by the relation

$$v = \frac{b\omega}{k}$$

where $1/k$ is the value that satisfied $I_{b\beta} = 0$. If the value of $R_{b\beta}'$ is exceeded by $I_\beta/\pi\rho b^4$, the control surface is being operated past the transition point and in the unstable region.

Flutter of control surface with structural damping in incompressible flow.- As is often done, the type of damping force assumed is one that is inphase with the velocity $\dot{\beta}$ but proportional to the angular displacement β.

The results of computations for one location of the axis of rotation $c = 0.7$ are presented in figures 5 and 6. In figure 5, the flutter-speed parameter $v/b\omega_\beta$ is plotted against the inertia parameter. As noted, there is a very large effect of the damping parameter and it may be that structural damping could be used for eliminating this type of oscillation. In figure 6, the frequency ratio $(\omega/\omega_\beta)^2$ is plotted against the inertia parameter. It should be noted that flutter does not occur (contrary to the case for zero damping) at a constant value of the reduced speed $v/b\omega$ as the inertia parameter is varied. The values of $v/b\omega$ and $I_\beta/\pi\rho b^4$ for several values of the structural damping coefficient for $c = 0.7$ are as follows:

g_β	1/k for -				
	$\frac{I_\beta}{\pi\rho b^4} = 20$	$\frac{I_\beta}{\pi\rho b^4} = 30$	$\frac{I_\beta}{\pi\rho b^4} = 50$	$\frac{I_\beta}{\pi\rho b^4} = 75$	$\frac{I_\beta}{\pi\rho b^4} = 100$
0	34.25	34.25	34.25	34.25	34.25
.01	38.0	44.77	56.1	67.58	77.60
.02	38.80	46.36	58.8	71.50	82.35

Flutter of a control surface having aerodynamic balance and zero structural damping.- Calculations have been performed for two control surfaces by use of equations (8) and (9) for two locations of axis of rotation e but one value of c, and the results are plotted in figures 7 and 8. In figure 7 the flutter-speed coefficient is plotted against $I_\beta/\pi\rho b^4$ for $c = 0.4$ and $e = 0.55$ and $e = 0.75$. The curves are similar to those obtained without aerodynamic balance, except that the limiting value (vertical asymptote) appears to be at a larger value of the abscissa. In figure 8 the frequency ratio $(\omega/\omega_\beta)^2$ is plotted against the inertia parameter $I_\beta/\pi\rho b^4$ for the same cases.

The important facts to be noted are (1) that aerodynamic balance did not eliminate single-degree-of-freedom instability of a control surface and (2) that the greater the amount of aerodynamic balance, the higher the limiting value of the inertia parameter at which the oscillation could begin for this particular case.

Flutter of control surface in compressible flow.- The results of the calculations based on the equations and tables discussed earlier are presented in figures 9, 10, and 11. In figure 9 the flutter-speed parameter is plotted against the inertia parameter for $M = 0$, 0.7, and 10/9. The curves for $M = 0.7$ and $M = \frac{10}{9}$ are similar in form to the curve for $M = 0$, except that the stable range of the inertia parameter is greatly reduced as the Mach number is increased. Another effect of increasing Mach number is to reduce the value of the reduced-velocity coefficient $1/k$, and this reduction is believed to be significant. In figure 10 the frequency ratio is plotted against the inertia parameter for three Mach numbers $M = 0$, 0.7, and 10/9.

A significant plot is made when the asymptotic value of the inertia parameter is plotted against Mach number as shown in figure 11. The relation between the inertia parameter and Mach number appears to be linear, and the region to the right and above the curve is the unstable range. This plot, as discussed earlier, is of particular significance with regard to the control surface without elastic restraint ($\omega_\beta = 0$) and shows that an aileron that is stable in the low Mach number range could become unstable in the high subsonic or lower supersonic range.

The asymptotic value of the inertia parameter at $M = 0.7$ for several positions of the control-surface hinge axis is included in figure 4. The effect of Mach number is again apparent in that increasing Mach number considerably reduced the value of the inertia parameter for a given hinge position at which oscillation could occur.

VARIOUS PRACTICAL LIMITATIONS TO THEORY

In general, theoretical control-surface derivatives (either steady or unsteady) have not always been in good agreement with experiment. This difference is even more pronounced at the higher aircraft flight speeds and is partially due to breakdown and separation of the flow over the rear part of the wing. Since the aerodynamic coefficients have been derived on the basis of nonviscous, linearized, potential flow for simplified models, and the actual flow is viscous, nonlinear, and nonpotential, the differences between theory and experiment are not unexpected. However, studies of control-surface characteristics based on potential-flow theory should provide a basis for the study of the separated-flow phenomena and provide for a logical grouping of the variables to be experimentally investigated.

The present calculations have been based on two-dimensional aerodynamic coefficients and hence do not take into account the effect of aspect ratio. Aspect ratio could have an appreciable effect on this

type of oscillation since, for the most part, the oscillations are of a low frequency and approach the range of stability frequencies. However, reference 6 shows that the effect of finite aspect ratio for a pitching wing in supersonic flow reduces but does not eliminate the instability, and a reasonable assumption is that a similar effect may be found for the subsonic case.

The influence of additional degrees of freedom was not considered in the analysis. Actual configurations will normally have more than one degree of freedom, but an analysis based on a single-degree-of-freedom system may be an easily obtained limit for cases of coupled flutter. There may, however, be circumstances in which only one degree of freedom is of importance. Cunningham (reference 3) showed in a recent paper that a slight relaxing of the condition of infinite stiffness of another degree of freedom did not appreciably influence the flutter speed.

Another factor which might be of importance is the thickness of the control surface. The aerodynamic coefficients used here were based on the concept of replacing the wing and control surface by an infinitely thin mean camber line. The effect of thickness requires further investigation.

CONCLUSIONS

Single-degree-of-freedom-flutter calculations which show the effects of various independent parameters, namely, Mach number, location of hinge axis, aerodynamic balance, and structural damping are presented for a control surface. The following conclusions may be enumerated:

1. Calculations based on unsteady potential-flow theory indicate the existence of single-degree-of-freedom flutter of a control surface.

2. Flutter of a control surface alone is more likely to occur for a configuration operating at high subsonic or low supersonic speeds and at high altitudes than at low speeds and low altitudes.

3. Structural damping has a beneficial effect, since it raises the flutter speed appreciably. The use of structural damping may be a convenient method of eliminating single-degree-of-freedom flutter.

4. The unstable oscillation is still possible if the control surface is aerodynamically balanced.

5. These results have several practical limitations. Such effects as separated flow, aspect ratio, coexistence of other degrees of freedom, and finite thickness of control surface were not considered and could be significant. However, the results should prove useful as a basis for further experimental study.

Langley Aeronautical Laboratory
National Advisory Committee for Aeronautics
Langley Field, Va., August 17, 1951

REFERENCES

1. Smilg, Benjamin: The Instability of Pitching Oscillations of an Airfoil in Subsonic Incompressible Potential Flow. Jour. Aero. Sci., vol. 16, no. 11, Nov. 1949, pp. 691-696.

2. Runyan, Harry L.: Single-Degree-of-Freedom-Flutter Calculations for a Wing in Subsonic Potential Flow and Comparison with an Experiment. NACA TN 2396, 1951.

3. Cunningham, Herbert J.: Analysis of Pure-Bending Flutter of a Cantilever Swept Wing and Its Relation to Bending-Torsion Flutter. NACA TN 2461, 1951.

4. Garrick, I. E., and Rubinow, S. I.: Flutter and Oscillating Air-Force Calculations for an Airfoil in a Two-Dimensional Supersonic Flow. NACA Rep. 846, 1946. (Formerly NACA TN 1158.)

5. Temple, G., and Jahn, H. A.: Flutter at Supersonic Speeds. Part I. Mid-Chord Derivative Coefficients for a Thin Aerofoil at Zero Incidence. R. & M. No. 2140, British A.R.C., 1945.

6. Watkins, Charles E.: Effect of Aspect Ratio on Undamped Torsional Oscillations of a Thin Rectangular Wing in Supersonic Flow. NACA TN 1895, 1949.

7. Smilg, Benjamin: The Prevention of Aileron Oscillations at Transonic Airspeeds. AAF TR No. 5530, Materiel Command, Army Air Forces, Dec. 24, 1946.

8. Theodorsen, Theodore: General Theory of Aerodynamic Instability and the Mechanism of Flutter. NACA Rep. 496, 1935.

9. Theodorsen, Theodore, and Garrick, I. E.: Nonstationary Flow about a Wing-Aileron-Tab Combination Including Aerodynamic Balance. NACA Rep. 736, 1942. (Formerly NACA ARR, March 1942.)

10. Dietze, F.: The Air Forces of the Harmonically Vibrating Wing in a Compressible Medium at Subsonic Velocity (Plane Problem). Part II: Numerical Tables and Curves. Translation No. F-TS-948-RE, Air Materiel Command, U. S. Air Force, March 1947.

11. Turner, M. J., and Rabinowitz, S.: Aerodynamic Coefficients for an Oscillating Airfoil with Hinged Flap, with Tables for a Mach Number of 0.7. NACA TN 2213, 1950.

12. Huckel, Vera, and Durling, Barbara J.: Tables of Wing-Aileron Coefficients of Oscillating Air Forces for Two-Dimensional Supersonic Flow. NACA TN 2055, 1950.

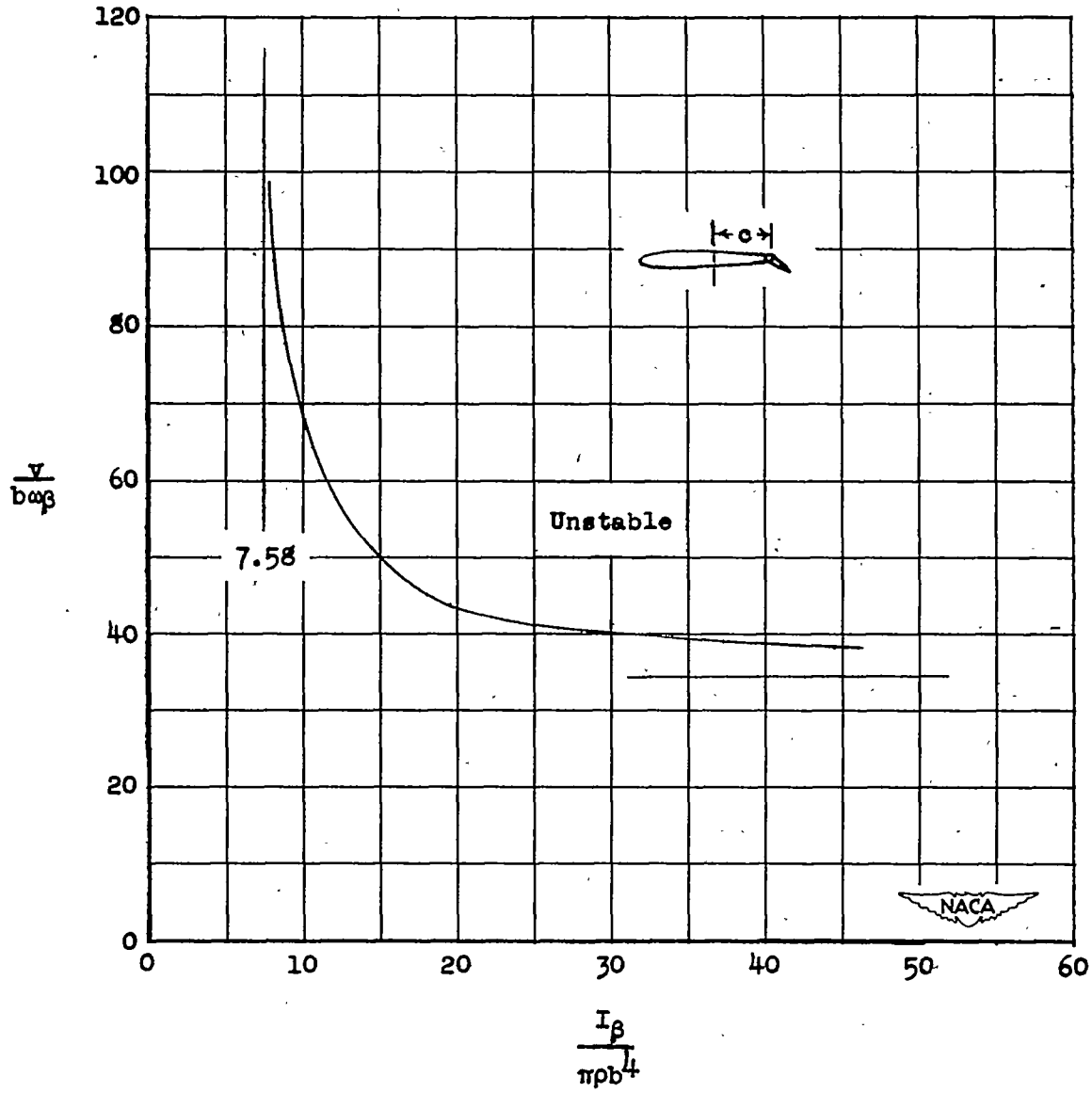

(a) c = 0.8.

Figure 1.- Plot of flutter-speed parameter $\frac{V}{b\omega_\beta}$ against an inertia parameter $\frac{I_\beta}{\pi\rho b^4}$ for various axis-of-rotation locations of a control surface in incompressible flow.

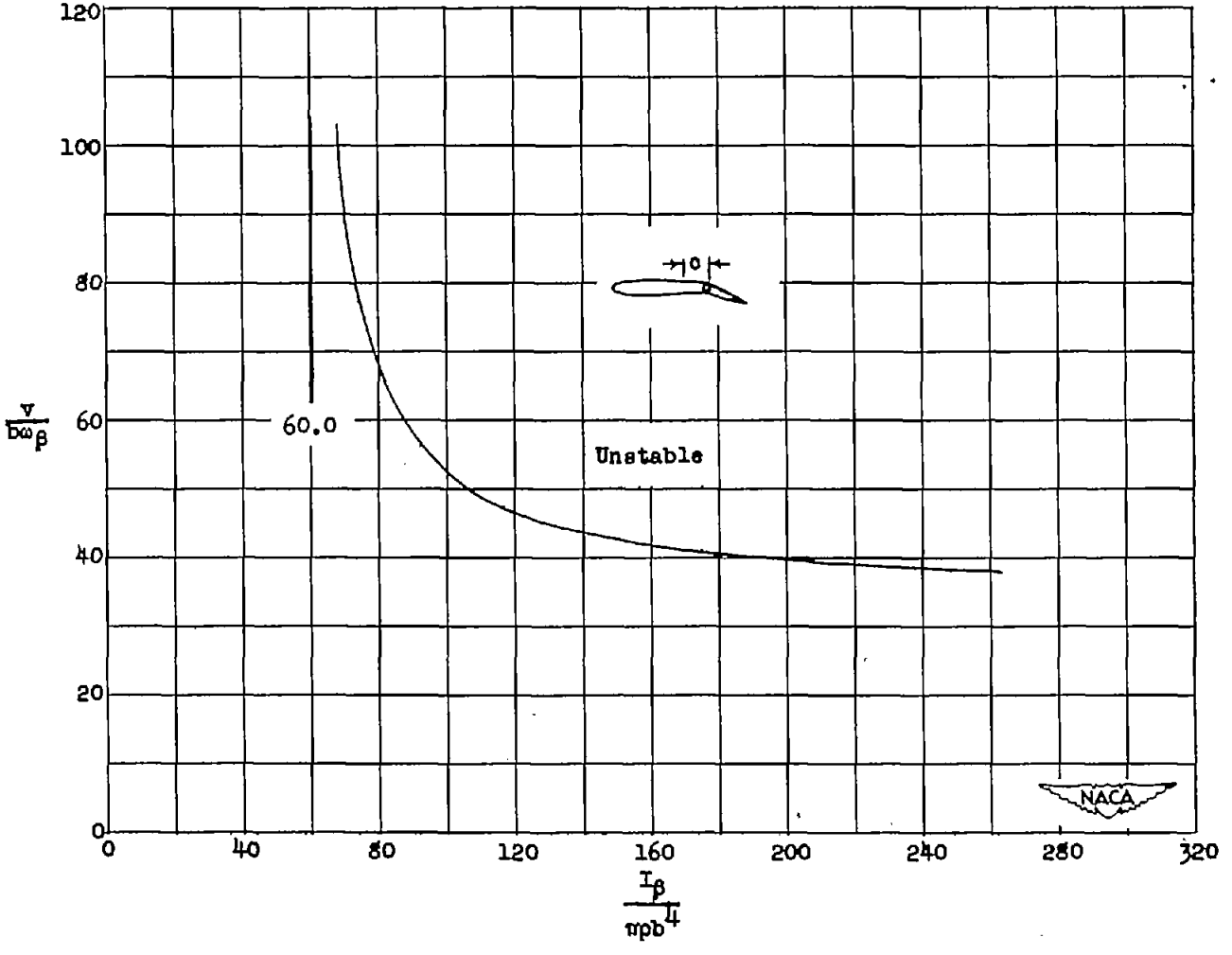

(b) $c_* = 0.4$.

Figure 1.- Continued.

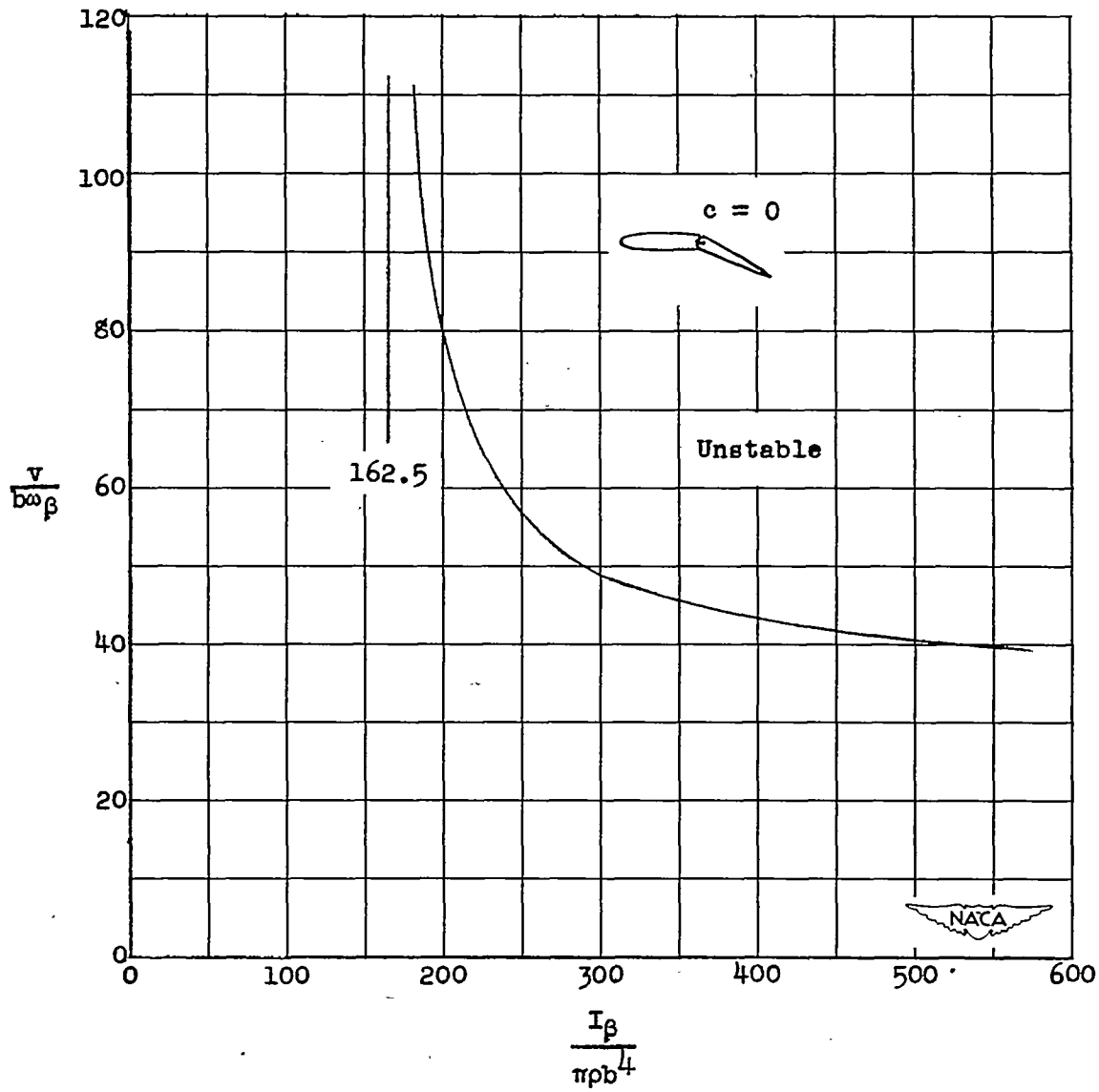

(c) c = 0.

Figure 1.- Continued.

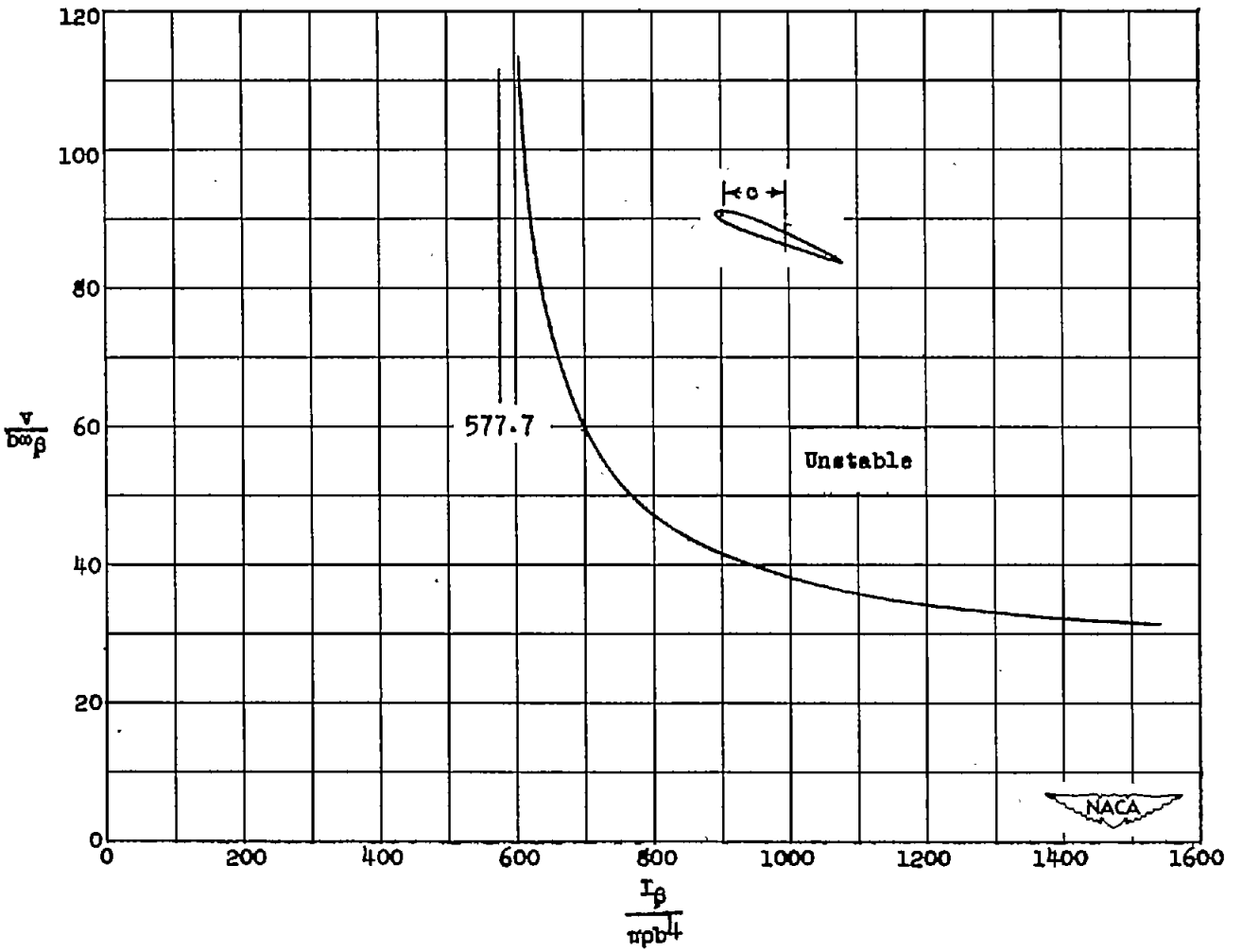

(d) c = -1.0.

Figure 1.- Concluded.

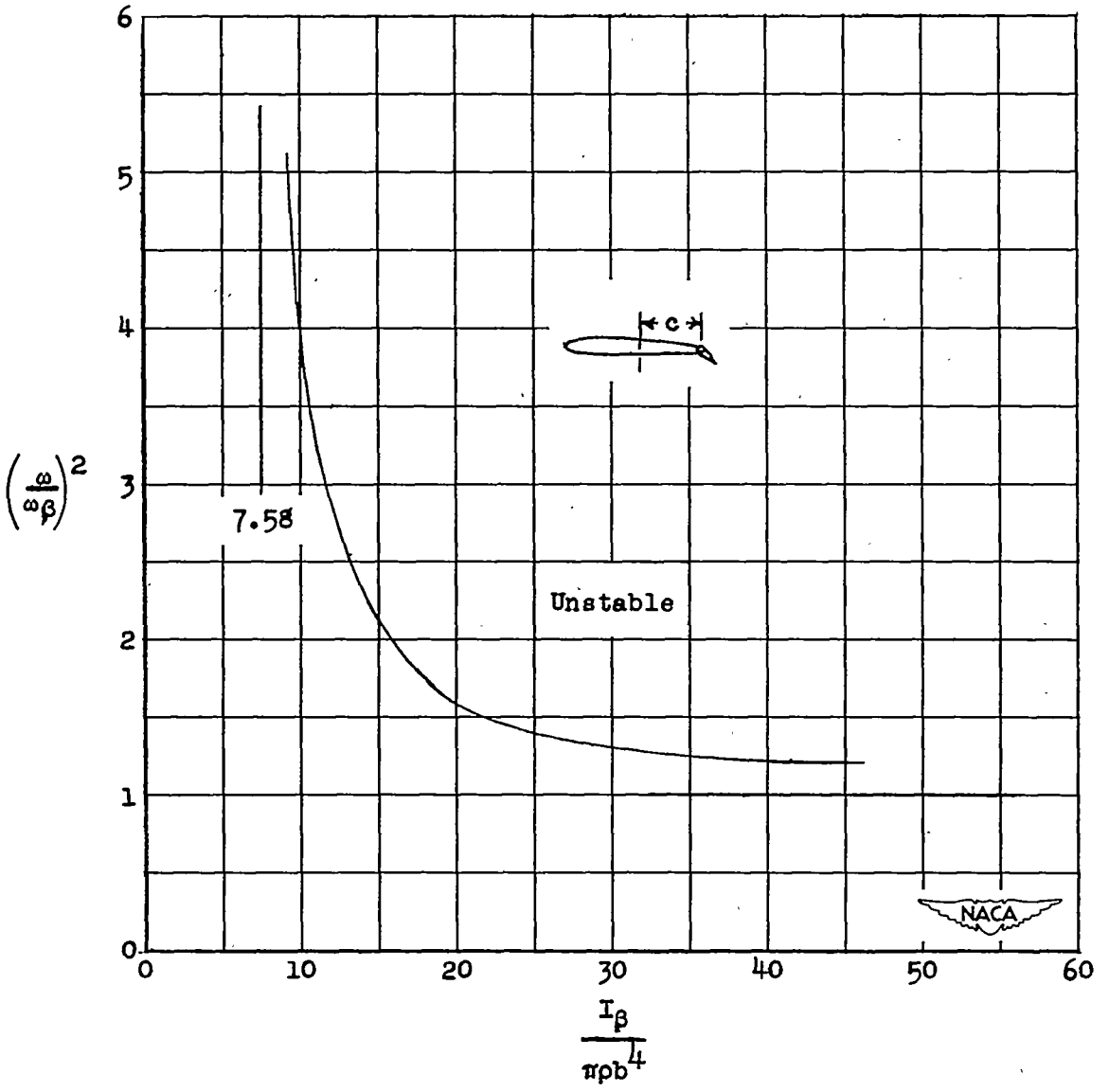

(a) c = 0.8.

Figure 2.- Plot of flutter-frequency ratio $\left(\frac{\omega}{\omega_\beta}\right)^2$ against an inertia parameter $\frac{I_\beta}{\pi\rho b^4}$ for various axis-of-rotation locations of a control surface in incompressible flow.

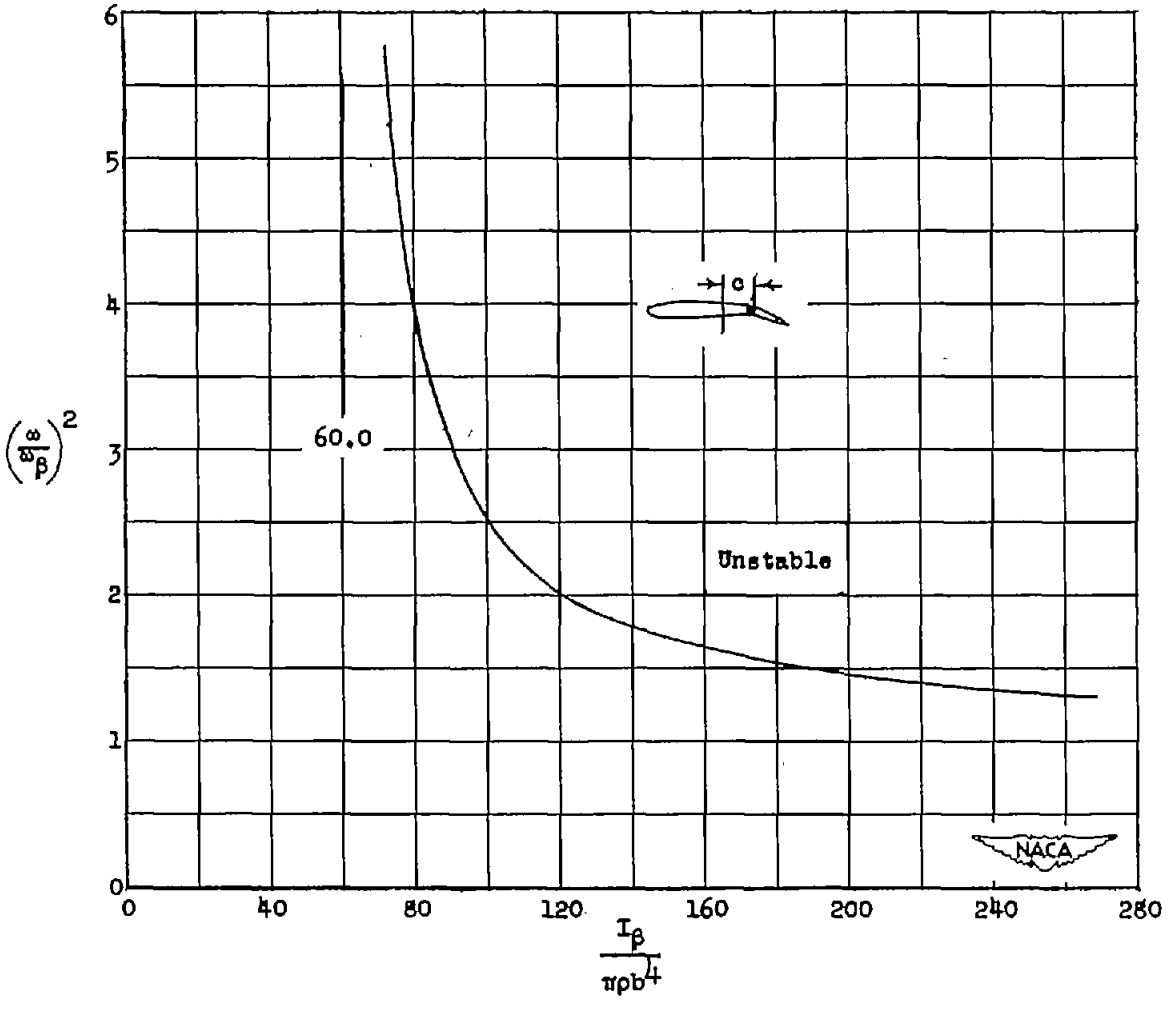

(b) c = 0.4.

Figure 2.- Continued.

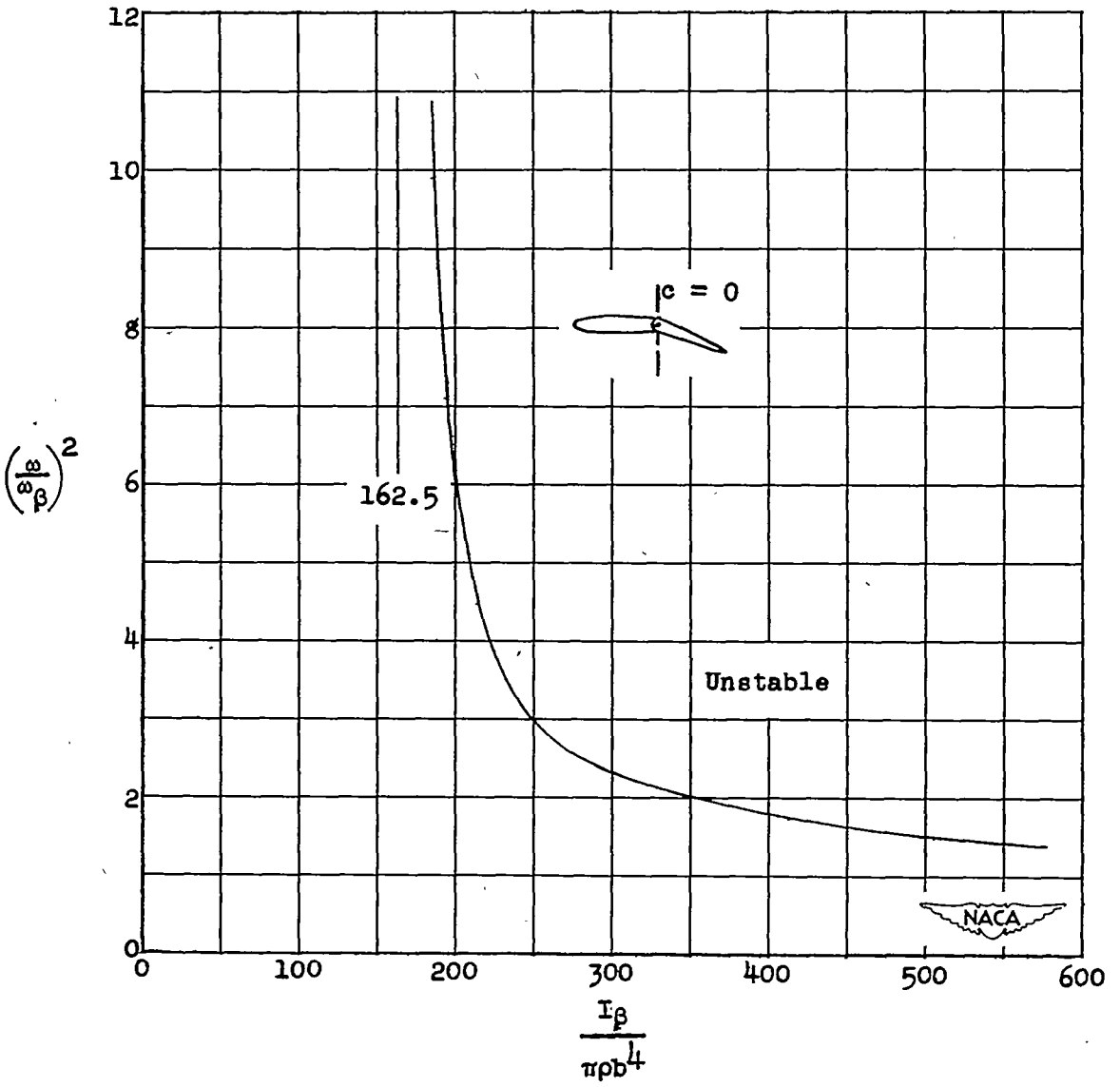

(c) c = 0.

Figure 2.- Continued.

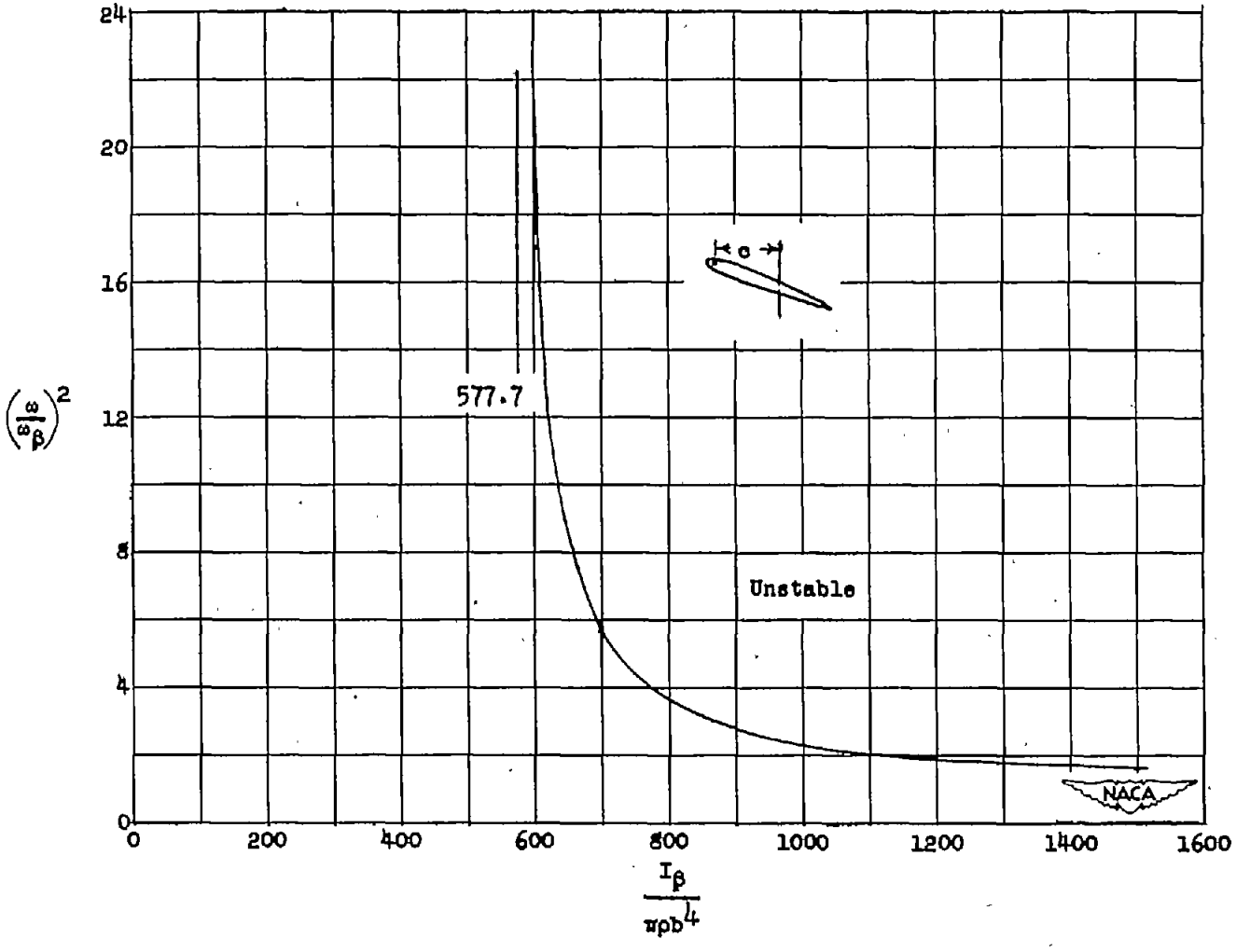

(d) c = -1.0.

Figure 2.- Concluded.

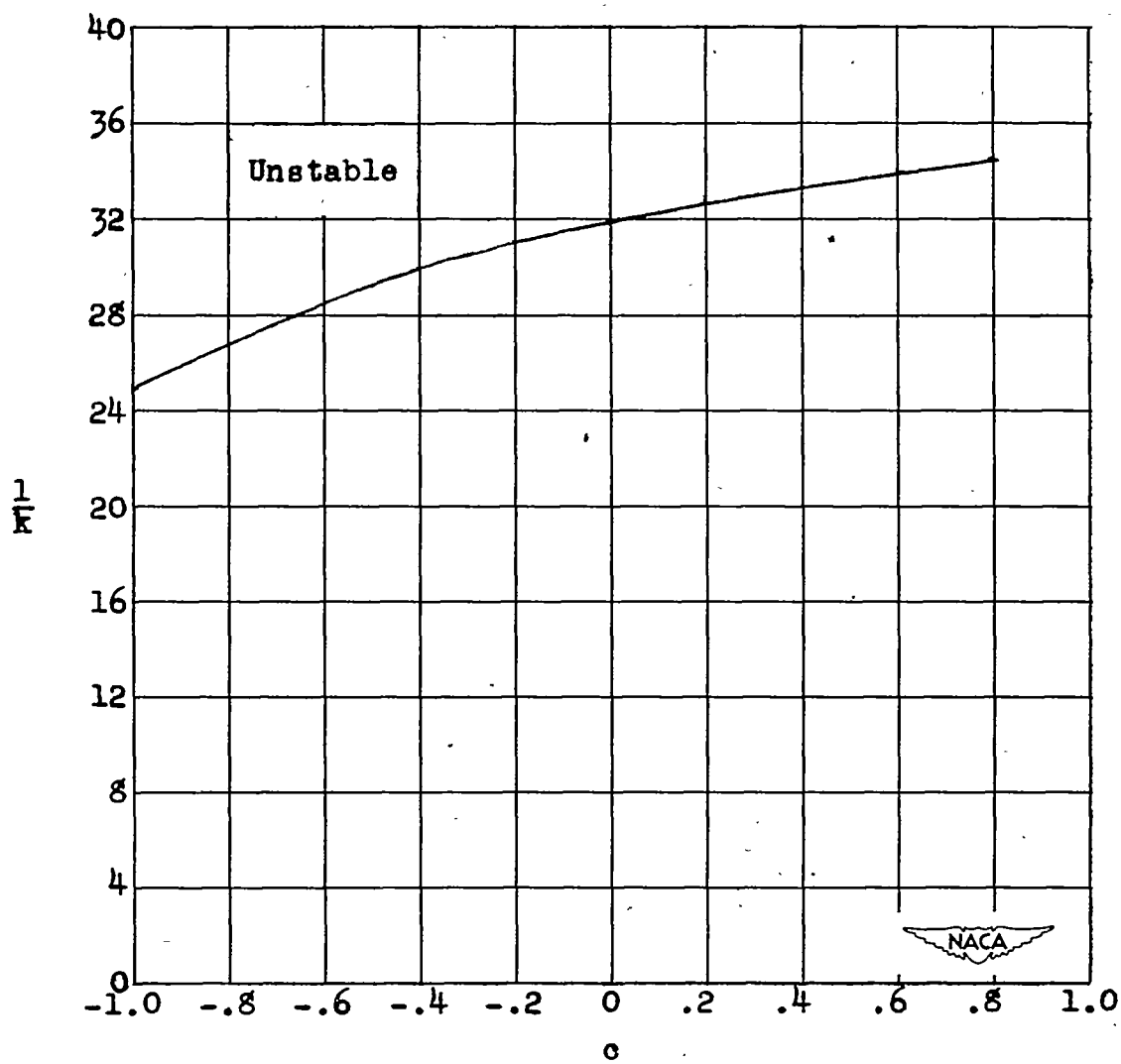

Figure 3.- Reduced velocity $1/k$ at which oscillation will occur plotted against location of control-surface axis of rotation c for incompressible flow.

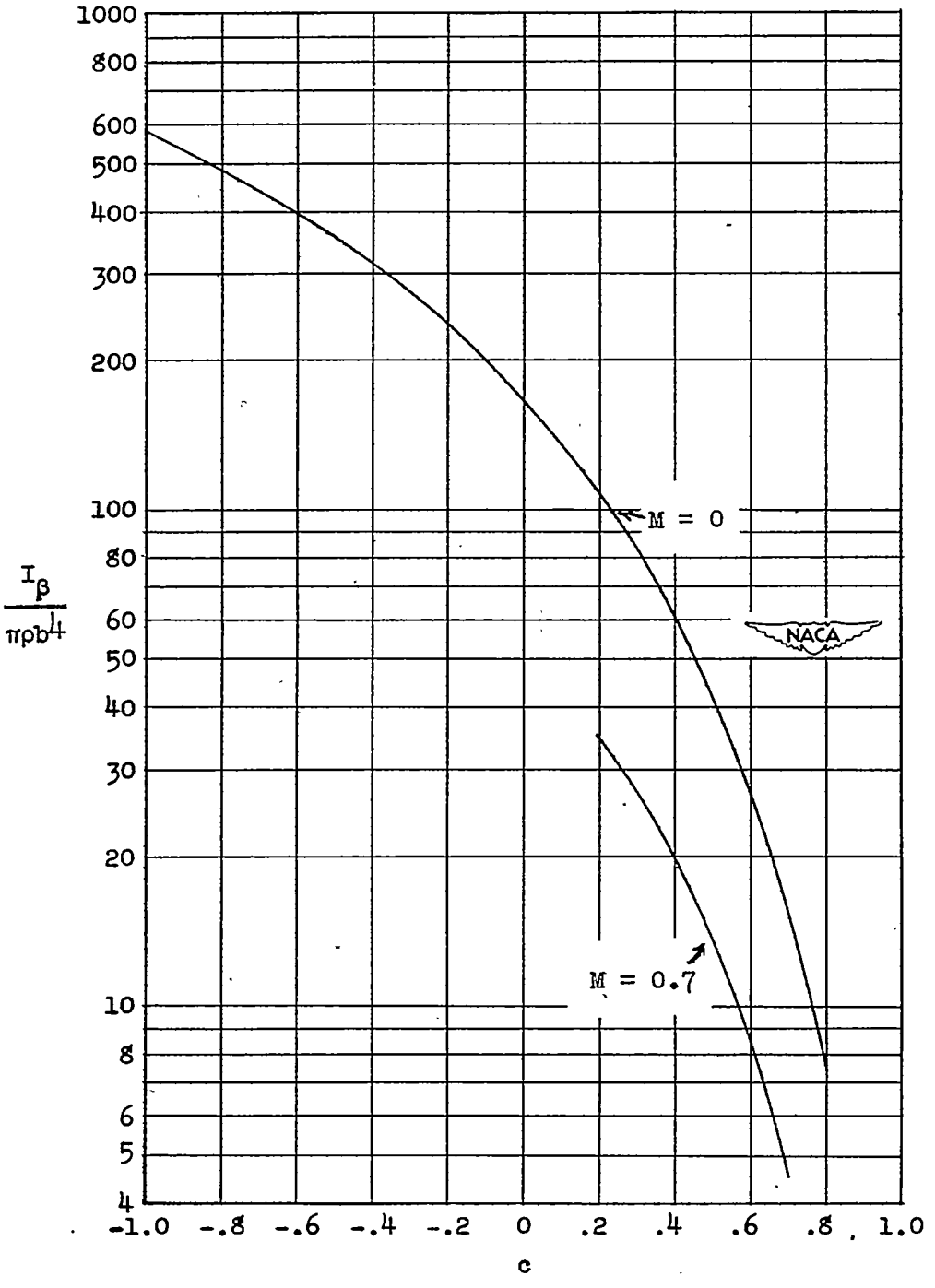

Figure 4.- Plot of asymptotic value of inertia parameter $\frac{I_\beta}{\pi\rho b^4}$ against location of control-surface axis of rotation c for M = 0 and M = 0.7.

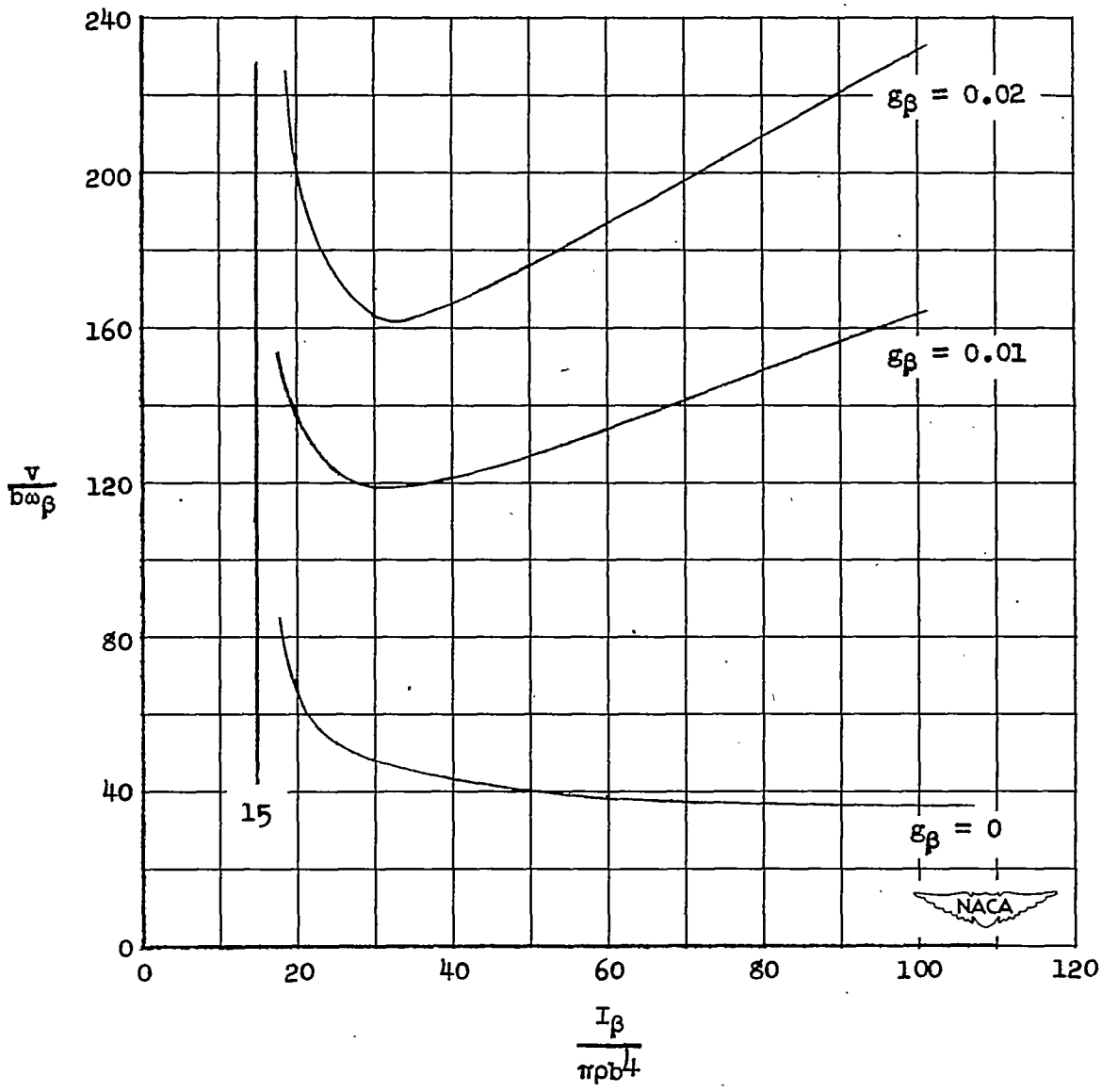

Figure 5.- Plots of flutter-speed parameter $\frac{v}{b\omega_\beta}$ against an inertia parameter $\frac{I_\beta}{\pi\rho b^4}$ for various values of structural damping g_β.

c = 0.7.

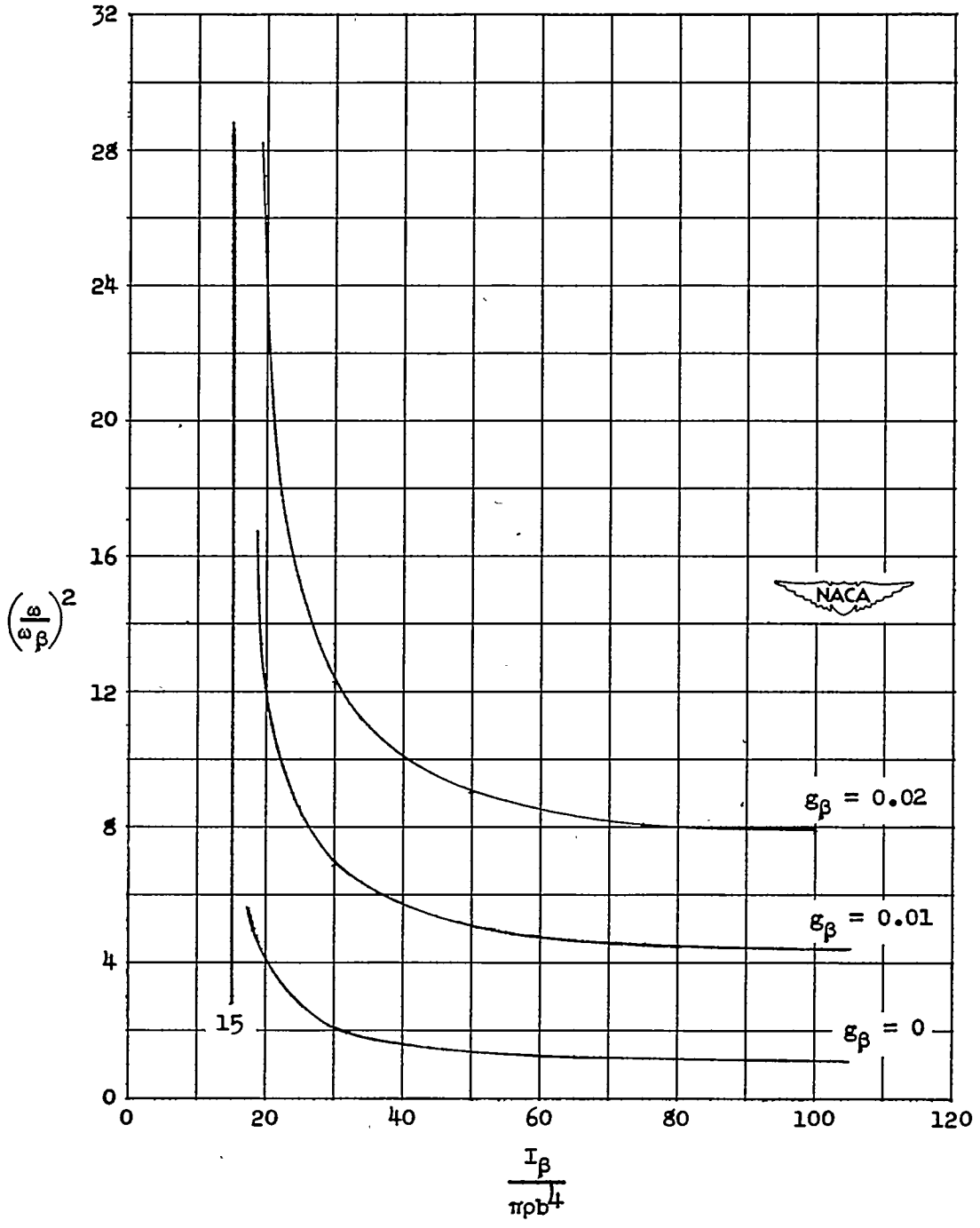

Figure 6.- Plots of frequency ratio $\left(\frac{\omega}{\omega_\beta}\right)^2$ against an inertia parameter $\frac{I_\beta}{\pi\rho b^4}$ for several values of structural damping g_β. c = 0.7.

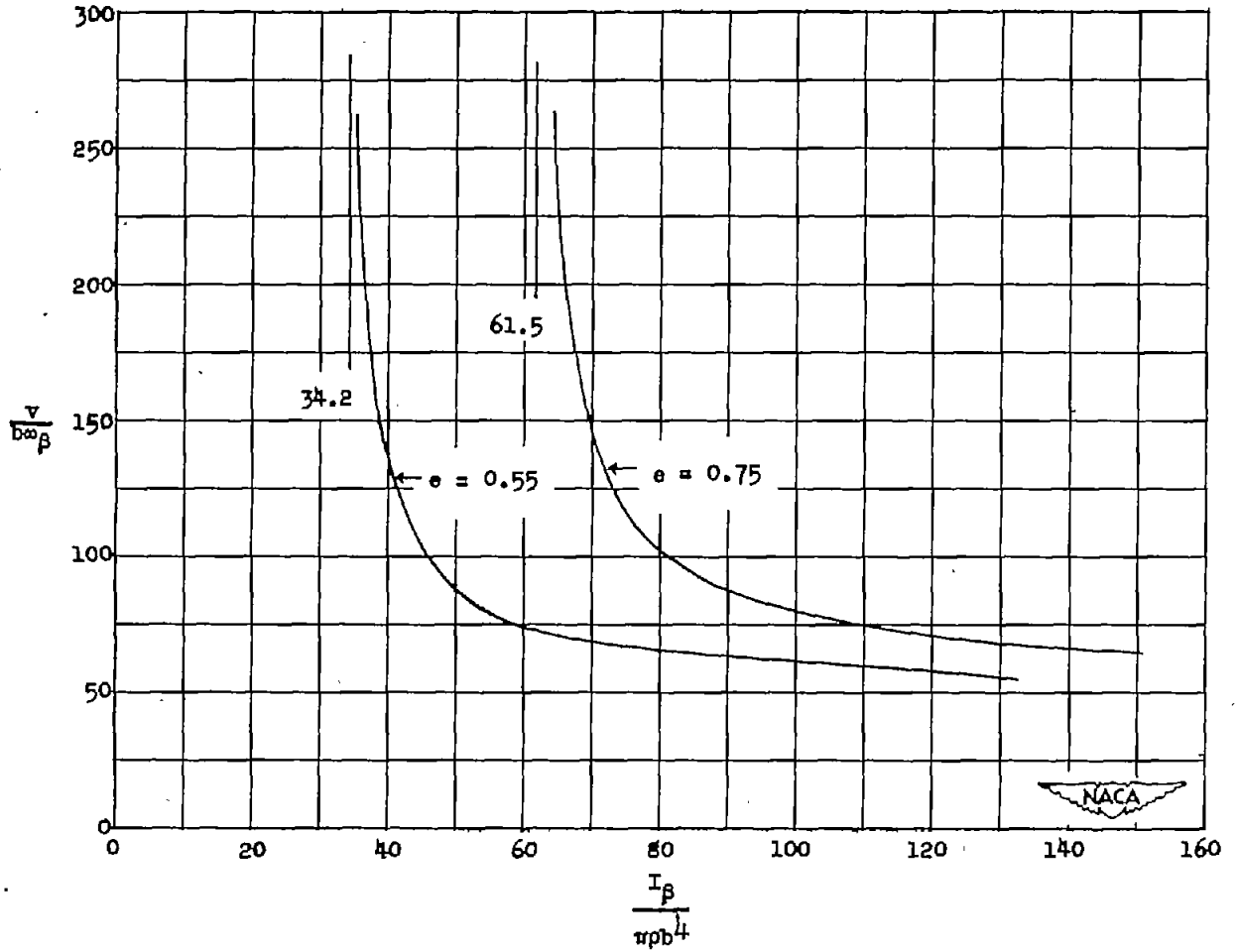

Figure 7.- Plot of flutter-speed parameter $\frac{V}{b\omega_\beta}$ against $\frac{I_\beta}{\pi\rho b^4}$ for two different amounts of aerodynamic balance. M = 0; c_l = 0.4.

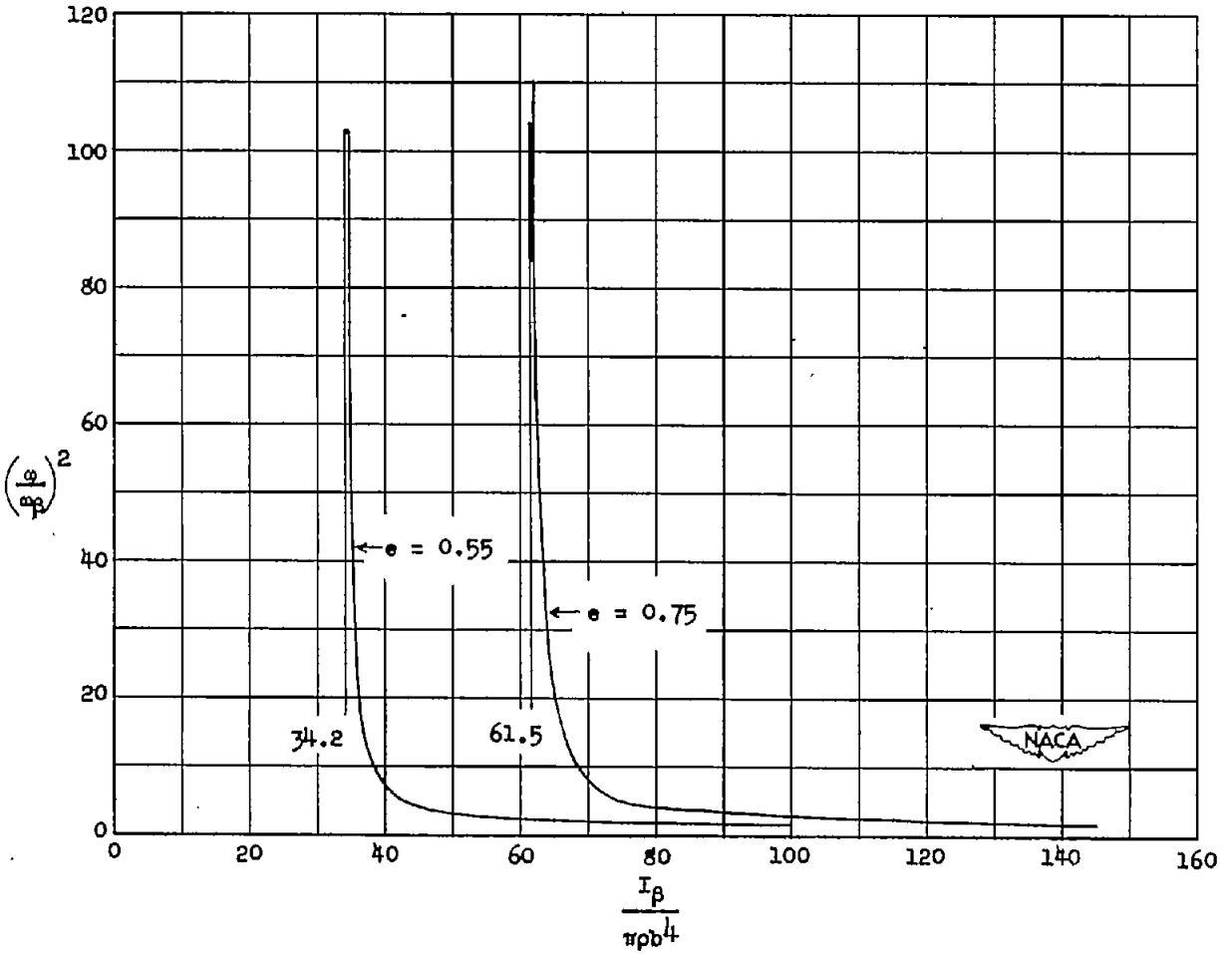

Figure 8.- Plots of $\left(\frac{\omega}{\omega_\beta}\right)^2$ against $\frac{I_\beta}{\pi\rho b^4}$ for two different amounts of aerodynamic balance. M = 0; c = 0.4.

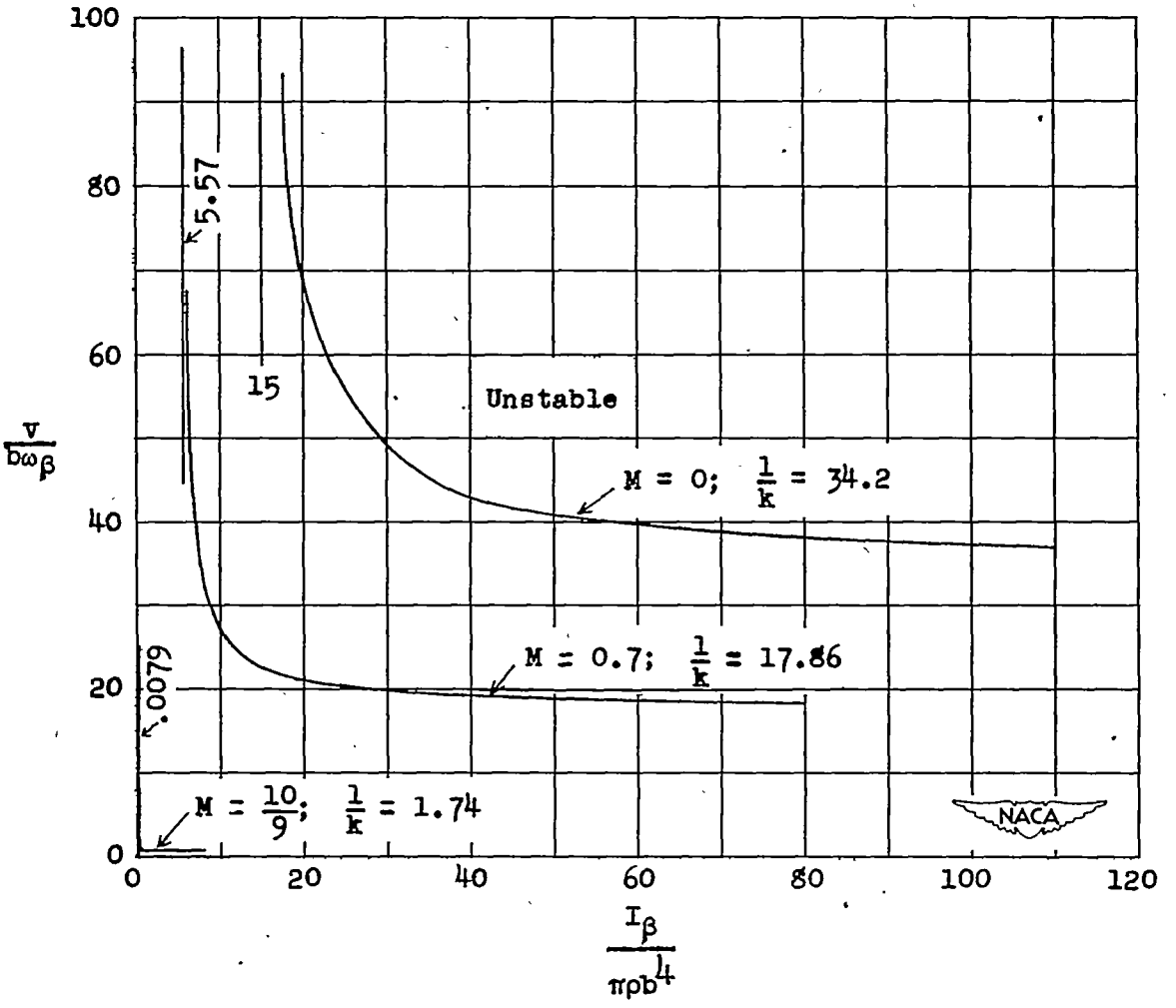

Figure 9.- Plot of flutter-speed parameter $\frac{v}{b\omega_\beta}$ against an inertia parameter $\frac{I_\beta}{\pi\rho b^4}$ for several values of Mach number M. c = 0.7.

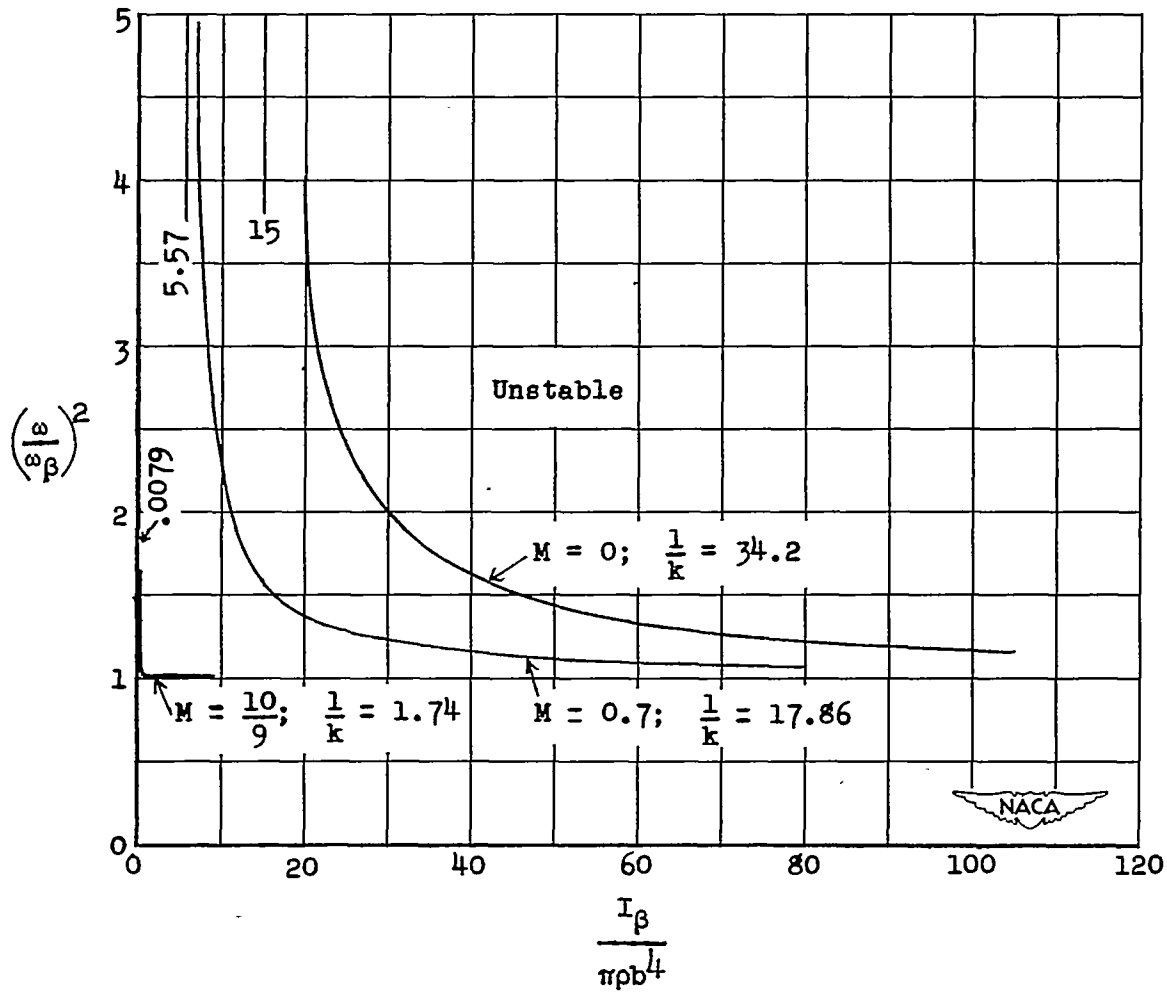

Figure 10.- Plot of frequency ratio $\left(\frac{\omega}{\omega_\beta}\right)^2$ against an inertia parameter $\frac{I_\beta}{\pi\rho b^4}$ for several values of Mach number M. c = 0.7.

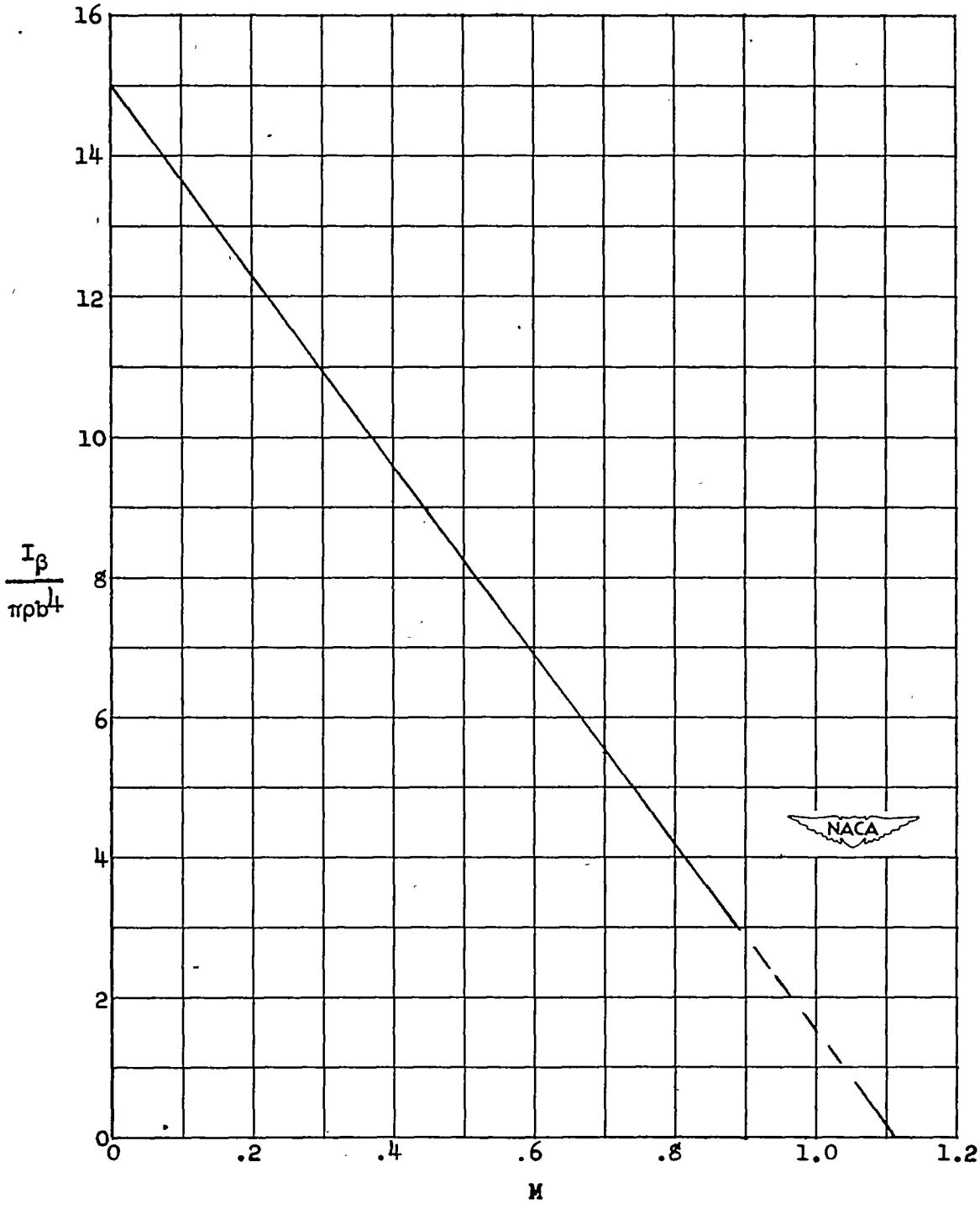

Figure 11.- Asymptotic value of inertia parameter $\frac{I_\beta}{\pi\rho b^4}$ against Mach number. $c = 0.7$.

NACA-Langley - 12-6-51 - 1000